

Stimulated Brillouin Scattering in High-Power Photonic Crystal Fiber Lasers in Different Pump Schemes

Abouricha M^{1*}, Boulezhar A¹, Amrane S² and Azami N²

¹Laboratory of Renewable Energy and System, Dynamics Faculty of Sciences Ain Chock, Hassan II University Casablanca, Morocco
²National Institute of Posts and Telecommunications, Rabat, Morocco

Abstract

We present in this paper the special structure of photonic crystal fiber (PCF), the temperature-dependent Yb³⁺ photonic crystal fiber lasers model with stimulated Brillouin scattering (SBS) is presented by solving the steady-state rate equations with the (SBS) in the linear cavity. The numerical results show that the pump power, laser power and Stokes powers propagating along axial positions are obtained by using the finite difference method and shooting method. The comparison results of the photonic crystal fiber laser model without temperature factor, the output powers and the SBS threshold powers in different pump schemes are obtained in the simulation paragraph. The numerical results show that the SBS threshold power in the two-end pump scheme is more noticeable than other pumps schemes.

Keywords: Stimulated Brillouin scattering; PCF; Fiber optic; Pump schemes

Introduction

Yb³⁺-doped photonic crystal fiber lasers pumped by laser diodes have more attracted attention in recent years, in several applications such as view commercial and military applications thanks to excellent beam quality, their high brightness, efficient heat dissipation, eminent efficiency, good compactness, etc., by comparison with traditional lasers such as solid-state or gas [1,2]. With the availability of high-power laser diode bars and clad-pumping techniques, the output power of YDDC fiber lasers is able to reach hundreds watts, even 1000 watt, in the regime of the continuous-waves (CW) [3-5]. But, the Extensibility of output powers can be limited by nonlinear processes and amplified spontaneous emission such as stimulated Raman scattering, the optical Kerr effect and stimulated Brillouin scattering (SBS). Although these nonlinear effects could be of interest for specific applications [6-9]. The maximum SBS threshold pump power is theoretically obtained by achieving high power output scalability and narrowing the line-width of the fiber laser, and 70% optical-optical efficiency was experimentally observed with 310W total pump power at 976 nm [10]. Due to the presence of the first-order Stokes waves initiated by forward and backward pump power, the output laser power increases slower with the increase of pump power under bidirectional end-pumping [11]. A numerical analysis of SBS in high power linear cavity Yb³⁺-doped double-clad fiber lasers is investigated, the SBS threshold power can be improved significantly by broadening laser line-width, effectively by using large mode area fiber, shortening cavity length and reducing input mirror reflectivity at Stokes wavelength [12]. In addition, the temperature factor has practically no effect on the corresponding laser output power to SBS threshold power [13], they can also lead to some unexpected instabilities in the laser signal. In particular, the SBS is expected to be the origin of instabilities in high-power fiber lasers [9] or deformation of pulses in fiber amplifiers [14]. The aim of this paper is to investigate theoretically the dependence of the SBS on system parameters in YDDC fiber lasers and the pumps schemes. By solving a set of laser rate equations with the SBS, the SBS thresholds are obtained under different fiber conditions. The results and analysis is presented facilitate the design and optimization of Yb³⁺-doped photonic crystal fiber lasers.

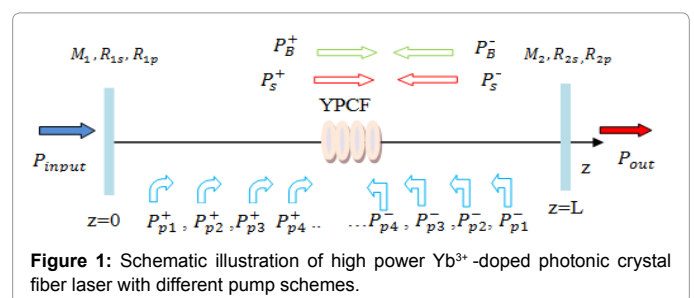
Theoretical Model

Pump schemes

The high power linear cavity Yb³⁺-doped fiber laser with SBS is described schematically in Figure 1. The rate rate equations with temperature factor in the steady-state [15] and SBS in high power Yb³⁺-doped fiber laser are described by the nonlinear coupled rate Equations. (1)–(4). In our numerical model, Yb³⁺-doped fiber laser, signal stimulated emission and absorption, stimulated emission at the pump wavelength and scattering losses; both for the pump and signal the are considered; but excited state absorption (ESA) and spontaneous emission are negligible, for high pumping conditions [16,17].

Rate equations with the SBS

$$N_2(z) = \frac{\frac{\Gamma_p \lambda_p^2 \sigma_{ap} J_p}{hcA} [P_p^-(z) + P_p^+(z)] + \frac{\Gamma_s \lambda_s^2 \sigma_{as} J_s}{hcA} [P_s^-(z) + P_s^+(z)]}{\frac{\Gamma_p \lambda_p^2 (\sigma_{ap} J_p + \sigma_{ep} J_{up})}{hcA} [P_p^-(z) + P_p^+(z)] + \frac{\Gamma_s \lambda_s^2 (\sigma_{as} J_s + \sigma_{es} J_{us})}{hcA} [P_s^-(z) + P_s^+(z)] + \frac{J_{sp}}{\tau}} \quad (1)$$



*Corresponding author: Abouricha M, Laboratory of Renewable Energy and System, Dynamics Faculty of Sciences Ain chock, Hassan II University Casablanca, Morocco, Tel: 06 14 000 400; E-mail: mmabouricha@gmail.com

Received November 22, 2017; Accepted December 04, 2017; Published December 20, 2017

Citation: Abouricha M, Boulezhar A, Amrane S, Azami N (2017) Stimulated Brillouin Scattering in High-Power Photonic Crystal Fiber Lasers in Different Pump Schemes. J Laser Opt Photonics 4: 170. doi: 10.4172/2469-410X.1000170

Copyright: © 2017 Abouricha M, et al. This is an open-access article distributed under the terms of the Creative Commons Attribution License, which permits unrestricted use, distribution, and reproduction in any medium, provided the original author and source are credited.

$$\pm \frac{dP_s^\pm(z)}{dz} = \Gamma_s [(\sigma_{as}f_{ls} + \sigma_{es}f_{us})N_2(z) - \sigma_{as}f_{ls}N]P_s^\pm(z) - \alpha_s P_s^\pm(z) - \frac{g_B}{A_{eff}} P_B^\pm(z)P_s^\pm(z) \quad (2)$$

$$\pm \frac{dP_p^\pm(z)}{dz} = \Gamma_p [(\sigma_{ap}f_{lp} + \sigma_{ep}f_{up})N_2(z) - \sigma_{ap}f_{lp}N]P_p^\pm(z) - \alpha_p P_p^\pm(z) \quad (3)$$

$$\pm \frac{dP_B^\pm(z)}{dz} = -\alpha_B P_B^\pm(z) + \frac{g_B}{A_{eff}} P_B^\pm(z)P_s^\pm(z) \quad (4)$$

Where:

$N_2(z)$ is the upper level population density, N is the total doping population density of Yb ions.

$P_p^\pm(z)$, $P_s^\pm(z)$ and $P_B^\pm(z)$ are the signal power, laser pump power and first-order Brillouin Stokes power along the fiber, respectively. λ_s and λ_p are the laser signal and pump wavelengths, respectively.

The minus - and plus + superscripts represent propagation along the negative or positive z-direction, respectively. Γ_p and Γ_s are the pump filling factor and laser signal filling factor in the fiber core, respectively. The expressions of these factors are the following:

$$\Gamma_s = 1 - \exp\left(-\frac{2a^2}{\omega^2}\right)$$

$$\Gamma_p = a^2 / b^2$$

Where ω is the field radius, b and a are the radius of the fiber core and inner cladding.

$\frac{\omega}{a} \approx 0.65 + 1.619V^{-\frac{3}{2}} + 2.879V^{-6}$ [18,19]. σ_{es} and σ_{as} are the emission cross-section and laser signal absorption, respectively. σ_{ep} and σ_{ap} are the emission cross-section and pump absorption, respectively. The scattering losses for the laser signal and pump powers are given by α_s and α_p , respectively. The value of α is less than 0.1 nm away from the laser wavelength therefore, $\alpha = \alpha_s h, c, \tau$ and A are the Planck's constant, light velocity spontaneous lifetime and Yb³⁺-doped area, respectively. g_B is the SBS gain, $g_B = g_0 \Delta\nu_B / (\Delta\nu_B + \Delta\nu_s)$, where g_0 , $\Delta\nu_B$ and $\Delta\nu_s$ are the intrinsic SBS gain constant, SBS gain bandwidth and laser bandwidth [18]. The effective core area A_{eff} is defined as πr^2 . $f_s(f_{lp})$ and $f_{us}(f_{up})$ are the Boltzmann occupation factor within upper and lower manifolds for the upper and lower levels of the laser (pump) transition [16,20]. At the pump wavelength $\lambda_p = 975$ nm and signal wavelength $\lambda_s = 1080$ nm, $f_{ls}(f_{lp})$ and $f_{us}(f_{up})$ are shown in Figure 2 and defined as follows:

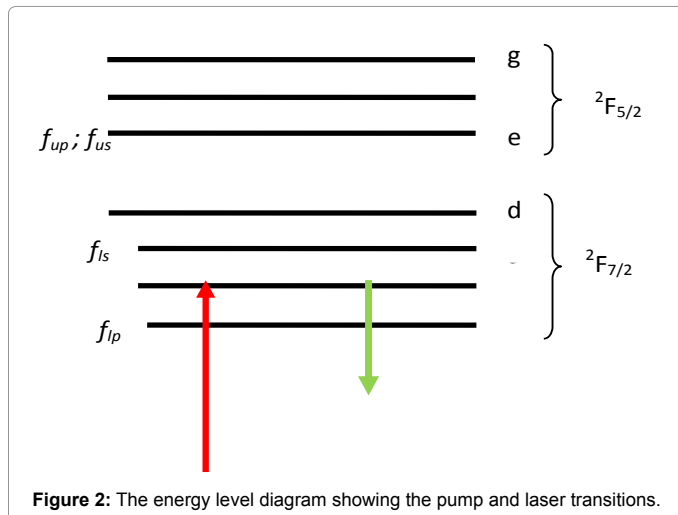


Figure 2: The energy level diagram showing the pump and laser transitions.

• Yb excited state:

$$f_{us} = f_{up} = \frac{\exp(-\frac{E_e}{kT})}{\sum_{x=a}^g \exp(-\frac{E_x}{kT})} \quad (5)$$

• Yb ground state:

$$f_{lp} = \frac{\exp(-\frac{E_a}{kT})}{\sum_{x=a}^d \exp(-\frac{E_x}{kT})} \quad (6)$$

• and:

$$f_{ls} = \frac{\exp(-\frac{E_c}{kT})}{\sum_{x=a}^d \exp(-\frac{E_x}{kT})} \quad (7)$$

Where:

E_x is the energy level difference between levels x and a in the Yb ground state and excited state, as shown in Table 1 [21,22].

k is the Boltzmann constant; T is the temperature distribution in the fiber core area, expressed by the following [23]:

$$T(r) = T_0 - \frac{Q(z)r^2}{\pi k_1} \quad \text{if } (0 \leq r \leq a) \quad (8)$$

Where T_0 represents the temperature of fiber axis ($r=0$), k_1 is the thermal conductivity of material and T_c is the environment temperature, such as $T_c = 298$ K, h_c is the heat transmission coefficient of the fiber surface and denotes thermal conductivity. a and b are the radius of the fiber core and fiber outer cladding. $Q(z)$ is the heat power density, defined as [15]:

$$Q(z) = \frac{\alpha(z) [P_p^+(z,t) + P_p^-(z,t)]}{\pi a^2} (1 - S) \quad (9)$$

Where $\alpha(z) = \alpha_a(z) + \alpha_p$, $\alpha_a(z)$ is absorption coefficient and S is the quantum efficiency whose theoretical value is λ_p/λ_s . However, it cannot reach the theoretical value in practical applications. In Other regions of the fiber, the value of $Q(z)$ is zero. Supposing perfect thermal connection among the inner-cladding and core, the temperature and their derivatives are continuous at the boundary ($r=a$). The two-point boundary conditions in the above model are

$$P_p^+(z=0) = P_{p01}, P_p^-(z=L) = R_{p2}P_p^-(z=L) \quad (10)$$

$$P_p^-(z=L) = P_{p02}, P_p^+(z=0) = R_{p1}P_p^+(z=0) \quad (11)$$

x	$E_x(\text{cm}^{-1})$	$\nu(\text{GHz})$	$h\nu(\text{J})$
g	11,630	348,900	2.3132E^{-19}
f	11,000	330,000	2.1879E^{-19}
e	10,260	307,800	2.0407E^{-19}
d	1490	44700	2.9636E^{-20}
c	1060	31800	2.1083E^{-20}
b	600	18000	2.1083E^{-20}
a	0	0	0

Table 1: Energy levels of Yb³⁺-doped fiber.

$$P_p^+(z=0) = P_{p01}, P_p^-(z=L) = P_{p02} \quad (12)$$

$$P_s^+(z=0) = R_{s1}P_s^-(z=0), P_s^-(z=L) = R_{s2}P_s^+(z=L) \quad (13)$$

$$P_B^+(z=0) = R_{B1}P_B^-(z=0), P_B^-(z=L) = R_{B2}P_B^+(z=L) \quad (14)$$

Simulation Results and Discussion

The data used in calculations are $\lambda_p=975 \text{ nm}$, $\lambda_s=1080 \text{ nm}$, $R_{is}=0.98$, $R_{2s}=0.04$, $L=5 \text{ m}$, $\tau=0.8 \text{ ms}$, $\sigma_{ap}=2 \times 10^{-24} \text{ m}^2$, $\sigma_{ep}=2 \times 10^{-24} \text{ m}^2$, $\Gamma_p=0.0012$,

$\sigma_{as}=3.1 \times 10^{-27} \text{ m}^2$, $\sigma_{es}=4.2 \times 10^{-25} \text{ m}^2$, $\Gamma_s=0.8$, $N=1.6 \times 10^{26}$, $\alpha_s=5 \times 10^{-3} \text{ m}^{-1}$, $\alpha_p=3.1 \times 10^{-3} \text{ m}^{-1}$ fiber core radius $D=10 \mu\text{m}$ and $NA=0.05$.

Note that bidirectional end-pumping, forward pump, forward pump with reflexion, backward pump and backward pump with reflexion are discussed. The forward pump power P_{p01} equal to the backward pump power P_{p02} in the simulation model. The laser output power P_s^{out} , backward Stokes power $P_B^-(z)$ and forward Stokes power $P_B^+(z)$ as a function of pump power with temperature factor at different pump schemes are depicted in Figure 3a-3e. The SBS occurs once the pump

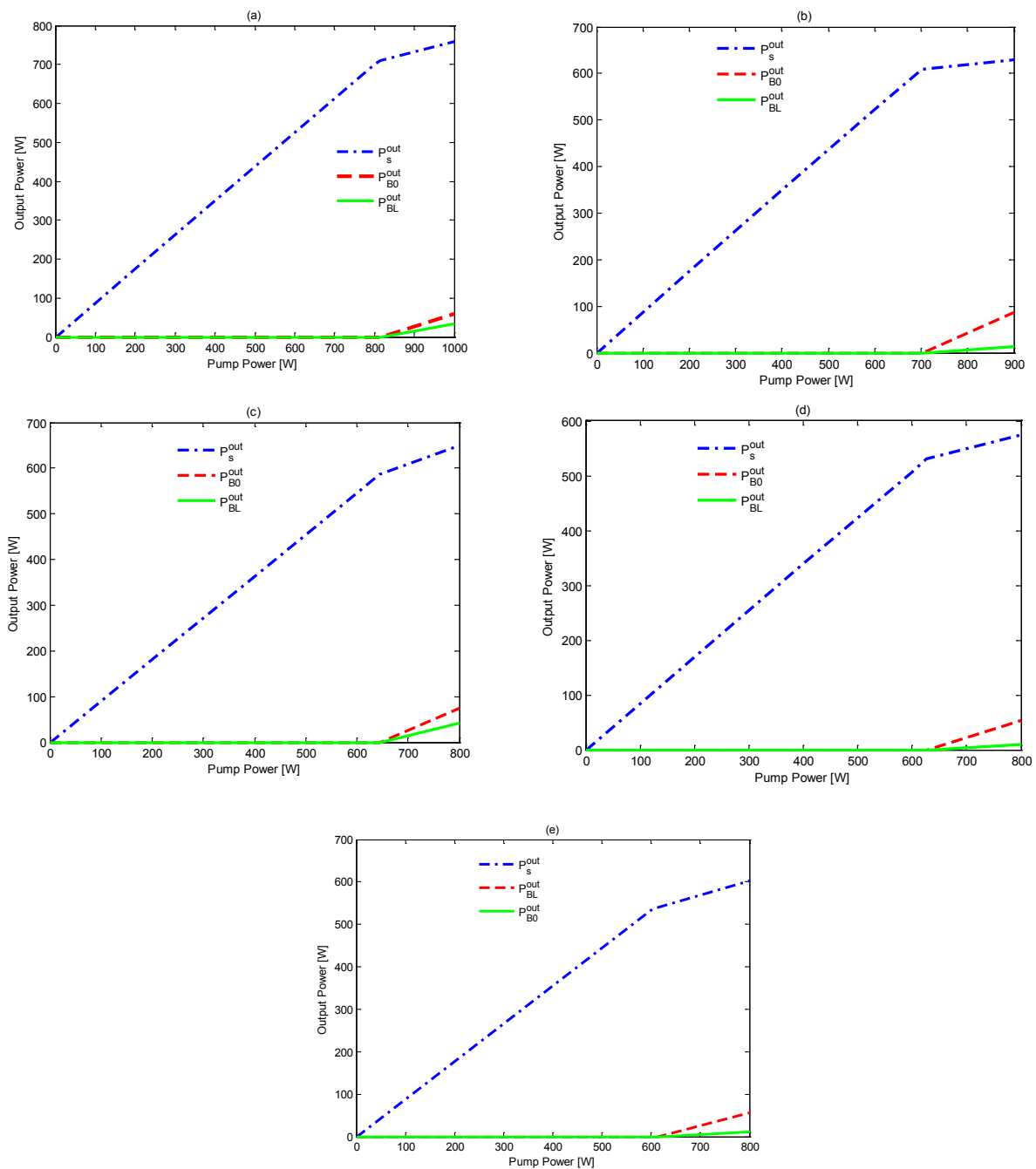
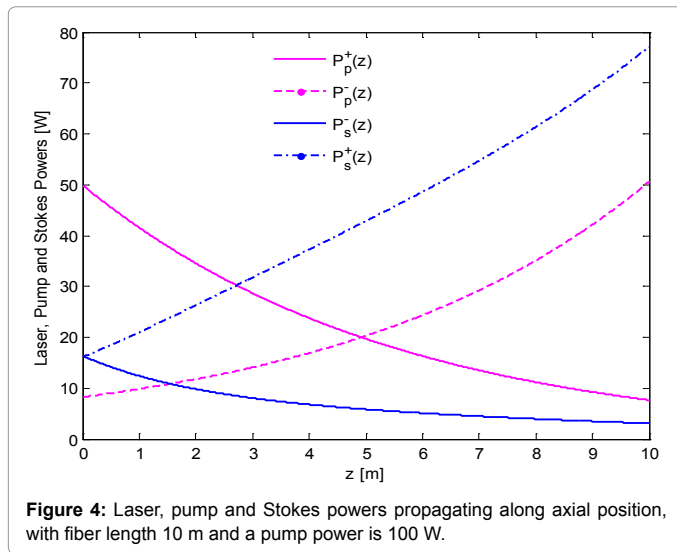


Figure 3: Output laser and Stokes power for different pump schemes: (a) Bidirectional pump scheme; (b) Forward pump scheme with $R_{p2}=0$; (c) Forward pump scheme with $R_{p2}=0.98$; (d) Backward pump scheme with $R_{p1}=0$; (e) Backward pump scheme with $R_{p1}=0.98$.



power reaches the Brillouin threshold power. When the pump power exceeds the Brillouin threshold power, the laser conversion efficiency starts to drop due to the presence of the forward and backward Stokes waves. The Brillouin threshold power and the corresponding laser output powers increases as the pump power increases. The Brillouin threshold powers considering temperature factor are respectively 825 W for the bidirectional pump scheme in Figure 3a, 702 W for the forward pump scheme without reflection in Figure 3b, 644 W for the forward pump scheme with reflection in Figure 3c, 627 W for the backward pump scheme without reflection in Figure 3d, and 612 W for the backward pump scheme with reflection in Figure 3e. In addition, the lasers outputs are correspondingly 771.63 W, 608.04 W, 536.02 W, 530.07 W and 540.31 W.

The pump power $P_p^\pm(z)$, signal power $P_s^\pm(z)$ and Stokes power $P_B^\pm(z)$ propagating along fiber axial position with bidirectional pump scheme and with pump power equal to 100 W, are shown in Figure 4. The Stokes power not appear, for the pump power of 100 W, because this value of the pump power not exceeds the threshold Stokes power.

Conclusion

The Stimulated Brillouin Scattering (SBS) of linear cavity high-power Yb³⁺-doped photonic crystal fiber lasers has been studied Numerically. By solving the rate equations with SBS, we have investigated the effects of pump schemes mode.

Numerical results show that the SBS threshold power can be improved significantly by the bidirectional pump scheme and the pump with reflectivity minimize the SBS threshold slightly in the both pump schemes forward and backward pump scheme with reflexion, compared with the both forward and backward pumps schemes respectively.

References

- DeLoach LD, Payne SA, Chase LL, Smith LK, Kway WL, et al. (1993) Evaluation of absorption and emission properties of Yb³⁺-doped crystals for laser applications. *IEEE J Quantum Electron* 29: 1179-1191

- Zenteno L (1993) High-power double-clad fiber lasers. *J Light wave Tech* 11: 1435-1446.
- Limpert J, Liem A, Zellmer H (2003) 500W continuous wave fiber laser with excellent beam quality. *Electron Lett* 39: 645-647.
- Jeong Y, Sahu JK, Baek S, Alegria C, Soh DBS, et al. (2004) Cladding-pumped ytterbium-doped large-core fiber laser with 610 W of output power. *Opt Commun* 234: 315-319.
- Jeong Y, Sahu J, Payne D, Nilsson J (2004) Ytterbium-doped large-core fiber laser with 1.36 kW continuous-wave output power. *Opt Express* 12: 6088-6092.
- Salhi M, Hideur A, Chartier T, Brunel M, Martel G, et al. (2002) Evidence of Brillouin scattering in an ytterbium-doped double-clad fiber laser. *opt Lett* 27: 1294-1296.
- Hideur A, Chartier T, Brunel M, Louis, S, Özkul C, et al. (2001) Generation of high energy femtosecond pulses from a side-pumped Yb-doped double-clad fiber laser. *Appl Phys Lett* 79: 3389-3391.
- Karpov VI, Dianov EM, Paramonov VM, Medvedkov OI, Bubnov MM, et al. (1999) Laser-diode-pumped phosphosilicate-fiber Raman laser with an output power of 1W 1.48 mm. *Opt Lett* 24: 887-889.
- Chen ZJ, Grudinin AB, Porta J, Minelly JD (1998) Enhanced Q switching in double-clad fiber lasers. *Opt Lett* 23: 454-456.
- Hekmat M, Dashhtabi M, Manavi S, Hassanpour E, Massudi R (2013) Study of the stimulated Brillouin scattering power threshold in high power double-clad fiber lasers. *Laser Phys* 23: 025104.
- Yang H, Duan K, Zhao B, Zhang E (2013) Theoretical study of stimulated Brillouin scattering in high-power dual-clad fiber lasers. *Optik* 124: 1049-1052.
- liu G, Liu D (2009) Numerical analysis of stimulated Brillouin scattering in high-power double-clad fiber lasers. *Optik* 120: 24-28.
- Hu X, Ning T, Chen Q, Li J (2015) Stimulated Brillouin scattering in Yb³⁺-doped dual-clad fiber lasers based on the temperature-dependent model. *optic* 126: 50-55.
- Hideur A, Chartier T, Ozkul C, Sanchez F (2000) Dynamics and stabilization of a high power side-pumped Yb doped double-clad fiber laser. *Opt Commun* 186: 311-317.
- Shimizu K, Horiguchi T, Koyamada Y (1992) Coherent light-wave amplification and stimulated Brillouin scattering in an erbium-doped fiber amplifier. *IEEE Photon Tech Lett* 4: 564-567.
- Shao H, Duan K, Zhu Y, Yan H, Yang H (2013) Numerical analysis of Ytterbium-doped double-clad fiber lasers based on the temperature-dependent rate equation. *Optik* 124: 4336-4340.
- Xiao L, Yan P, Gong M, Wei W, Ou P (2004) An approximate analytic solution of strongly pumped Yb-doped double-clad fiber lasers without neglecting the scattering loss. *Opt Commun* 230: 401-410.
- Marcuse D (1978) Gaussian approximation of the fundamental modes of graded-index fibers. *J Opt Soc Am B* 68: 103-109.
- Agrawal GP (2010) *Fiber-optic Communication Systems*, John Wiley & Sons, New York.
- Husein AHM, El-Astal AH, EL-Nahal FI (2011) The gain and noise figure of Yb-Er-codoped fiber amplifiers based on the temperature-dependent model. *Opt. Mater* 33 543-548.
- Peng X, Dong L (2008) Temperature dependence of ytterbium-doped fiber amplifiers. *J Opt Soc Am B* 25: 126-130.
- Brilliant NA, Lagonik K (2001) Thermal effects in a dual-clad ytterbium fiber laser. *Opt Lett* 26 1669-1671.
- Abouricha M, Boulezhar A, Habiballah NC (2013) The Comparative Study of the Temperature Distribution of Fiber Laser with Different Pump Schemes. *Open J Metal* 3: 64-71.